JJEE
Volume 8, Number 2, June 2022
Pages 179-194
Jordan Journal of Electrical Engineering
ISSN (Print): 2409-9600, ISSN (Online): 2409-9619

Development of a Droop Control Strategy for Flexible Operation of Distributed Generators

Salman Harasis[1*]

[1] Electrical Power and Mechatronics Engineering Department, Tafila Technical University, Tafila, Jordan
E-mail: salmanharasis@ttu.edu.jo

Received: February 02, 2022 *Revised: March 01, 2022* *Accepted: March 06, 2022*

***Abstract*—** Droop control is one of the control strategies utilized to establish a simple, effective, and a communication-less power sharing between several distributed generators (DGs) in power systems and microgrid networks. In this paper, the control of an inverter-based system operating with the proposed droop control is developed and analyzed. The proposed droop control with its adjustable nonlinearity level aims to flexibly control the DGs in order to fulfill multiple objectives that aim to stabilize the operation of the sources and optimize the power sharing. These objectives can be achieved, simultaneously, as the droop characteristics generated under the proposed control cover all the possible operating points in the frequency-active power ($f-P$) and voltage- reactive power ($V-Q$) planes. The capability of the proposed control strategy to construct highly non-linear characteristics enables the DG to effectively meet different complex technical and economic constraints. The work carried out in this paper focuses on the $f-P$ droop relation, and investigates the system performance under different physical and control parameters. The obtained results show that the proposed droop control is able to perform well under different operating conditions, shape the power sharing of the running DGs and stabilize the system performance.

***Keywords*—** Droop control; Distributed generation; Power sharing; Microgrid.

1. INTRODUCTION

In the recent decades, grid modernization has been effectively achieved in terms of transforming the conventional centralized power systems into distributed generation form. In addition, the smart grid concept introduces unique features to the grid [1, 2]. Therefore, flexible and reliable operation of all types of energy sources is now enabled. Microgrid networks - in both grid connected and islanded operating modes - are the main features of modernization where several economic, technical and environmental objectives can be effectively achieved. Therefore, large-scale deployment of microgrid networks can provide a potential solution to satisfy multiple objectives.

The droop control strategy is a well-known control technique that is inherited from the droop characteristics of the turbine-governor of the conventional control of synchronous generators [3]. This technique is widely used to control power-electronic interfaced microsources when working in parallel in power system applications. The droop control is a voltage control technique applied to the sources to construct a grid forming source able to stabilize the voltage and frequency. The implementation of the droop control as a local controller is widely adopted for its simplicity and reliability, and it does not require a communication system.

Different droop control strategies are discussed in literature. Linear droop control represents the simplest droop form where the droop coefficients are constant and determined based on the operating conditions of the sources [4]. Dynamic droop control is another droop

* Corresponding author
Article's DOI: 10.5455/jjee.204-1643827749

control type wherein the gains of the droop relation are adjusted online according to predetermined conditions and criteria set based on real time measurements. This type is a communication dependent where the communication may complicate the system, decrease the reliability and incur extra cost on the system budget. On the other hand, non-linear droop relation is adopted in some applications to combine the advantages of the linear and dynamic droop types. The non-linear droop characteristic is designed to fulfil technical and non-technical criteria that help achieving cost effective and reliable operation of the sources in the power system. Fig. 1 depicts the classification of the droop relations as discussed in literature.

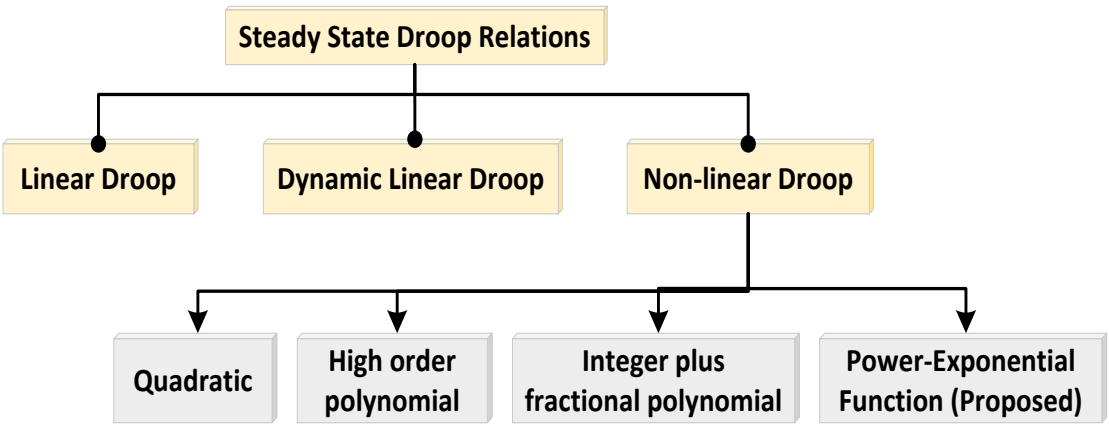

Fig. 1. Classification of the droop relations.

The authors in [5] proposed an adaptive droop control to properly achieve power sharing among distributed generators (DGs). The droop coefficients are adjusted according to the variable output power of renewable sources. The implementation of the control requires continuous estimation of the input power to change the droop coefficients. In [6], the authors developed a quadratic droop relation as a candidate controller for inverters in islanded microgrid. The controller has been implemented to achieve variable load sharing between the inverters to fulfil the stability requirements. The controller is supposed to be fed back continuously to update the fuzzy logic input that controls the value of the droop coefficient which imposes additional complexity on the system. The researchers in [7] proposed a tuneable droop control for stabilized operation of microgrid utilizing the particle swarm optimization and fuzzy logic control to schedule the appropriate gain under variable loading conditions. The controller is proposed to provide a virtual impedance to compensate for the line impedance and to improve the voltage regulation of the system. The authors in [8] proposed optimized frequency controllers using variable droop control for islanded microgrid to enhance the frequency stability of the network. The proposed scheme was considered to dynamically change droop coefficients. In [9], the researchers designed a fuzzy based generalized droop control for grid connected converters to, simultaneously, regulate the frequency and voltage. By implementing the control, the gains are adaptively updated to sustain the system stability under disturbances. The work carried out in [10] established a microgrid power flow using a fictitious slack bus to calculate the output power of the integrated DGs. The calculated power determined the droop coefficients under specific loading conditions and microgrid configuration. The authors in [11] proposed a constrained setting of the droop coefficients in islanded microgrids that are set based on the security of the

supply. The idea was to reduce the power interruptions at the expense of the voltage profile deterioration. The work in [12] discussed the implementation of high-order sliding mode controller, configured using Lyapunov function to reduce the reactive power sharing error among the DGs in small scale microgrid. The control is proposed as a nonlinear control able to compensate for the line impedances by constructing a variable virtual counter impedance. The controller proposed in [13] was found to improve both the accuracy of the reactive power sharing and voltage regulation during the steady state operation. The controller is a third order droop control that works to flatten the droop characteristics to minimize the voltage deviation against the increased reactive power sharing. However, the results showed bad transient behaviour of the power sharing profile.

The authors in [14] discussed an adaptive linear droop control strategy where the active power droop coefficient is tuned based on a decision made in the secondary control layer. The value of the coefficient is determined offline based on the cost minimization problem. In [15], the researchers investigated an improved droop control strategy for low voltage microgrids. A "sine droop" was proposed to mitigate coupling the active and reactive power sharing that appears due to the low X/R ratio. In [16], the authors examined the traditional droop control after adding a derivative term of the power signal command. This term keeps the steady state operation unchanged and significantly affects the transient power sharing of the sources. Therefore, transient power improvement was achieved by tuning the added term that controls the excess power sharing of small sources. The objectives of the proposed control strategy can be summarized as follows:

- It provides an adaptive power sharing capability that may change the loading of the DGs to stabilize the frequency and voltage under variable loading conditions.
- It is able to generate multiple linear and highly nonlinear droop characteristics. Therefore, it can be flat under light load and steep under heavy load to minimize the frequency and variation (Δf) and limits the power sharing.
- It can be easily implemented in any DG type; renewable source, battery, microturbine, etc., without the need to customize the characteristics that may be required to achieve multiple objectives.
- It can be configured offline or online. In offline, the coefficients can be determined according to predetermined system configuration, load profile, as well as the generation cost. In online, the controller can be tuned according to real time measurements to either control the amount the power supplied by the source or to regulate the voltage and frequency.
- The proposed control exhibits a manifold degree of freedom compared to linear droop, as changing (α_f , β_f)in $f - P$ and (α_v , β_v)in $V - Q$ droop relations shifts the droop characteristics horizontally and vertically at the same time.

2. EFFECTIVENESS OF THE DROOP MECHANISM BASED ON X/R RATIO

It is essential to mention that the ratio between the reactance and resistance, i.e., the X/R ratio is a major criterion in transient and steady state operation of a power system. In transient, X/R ratio determines the short circuit capacity of the system as the value of transient reactance (X') dictates the peak current. During steady state, X/R value dictates the decoupling between the active and reactive power sharing.

The droop relations can be divided into several types according to different criteria. The voltage level of the system indirectly reflects the suitable droop relation as the wiring system in each voltage level system has different X/R ratio as illustrated in Table 1. Practically, the suitability of the droop relation depends on the equivalent circuit of the system, X/R ratio of the lines and feeders and the output filters of the inverters. Therefore, an adequate decoupling - between the active and reactive powers - can be achieved to effectively control the system and manage the power flow [17-21]. The short circuit ratio (SCR) as defined in [22] is quantified as the ratio between the short circuit power to the system rating (S_{nom}) as a function of the ratio between X and R values. In other words, it represents the per unit short circuit capacity of the system. The SCR is expressed in the following equation [18, 22]:

$$SCR = \frac{P_{out}}{S_{nom}} = \frac{{V_{pcc}}^2}{S_{nom}(\sqrt{R^2+X^2})} \quad (1)$$

where P_{out}, S_{nom}, and V_{pcc} are the output power of the source, the nominal rating of the source in VA and the point of common coupling (PCC) voltage, respectively. In case when X/R is large, the coupling becomes largely inductive and an adequate active and reactive power decoupled control can be achieved. On the other hand, when X/R decreases, a resistive coupling exists, and the active and reactive power dynamics interact with each other. This, in turn, deteriorates the power sharing control and causes thermal problems. According to the complex source supplied power given in Eq. (2) and expressed in the source voltage (V_i) and the PCC voltage, the equations that govern the active and reactive powers are expressed in Eqs. (3) and (4), respectively where the expression after "≈ " sign is approximated considering a highly inductive coupling where δ is the source voltage angle [23-27].

$$S = VI^* = \frac{V_{pcc}V_i\angle\theta-\delta}{|Z|} - \frac{V_{pcc}^2\angle\theta}{Z} \quad (2)$$

$$P = [R\,cos(\delta) + X\,sin(\delta)]\frac{V_iV_{pcc}}{R^2+X^2} - \frac{V_{pcc}^2}{R^2+X^2}R \approx \frac{V_iV_{pcc}}{X}sin(\delta) \quad (3)$$

$$Q = [Xcos(\delta) - Rsin(\delta)]\frac{V_iV_{pcc}}{R^2+X^2} - \frac{V_{pcc}^2}{R^2+X^2}X \approx \frac{V_iV_{pcc}}{X}cos(\delta) - \frac{V_{pcc}^2}{X} \quad (4)$$

Table 1. X/R ratio for commonly used wiring system.

Voltage level	X/R [per km]
High voltage	≈ (3.5-6)
Medium voltage	≈(1.4-3.5)
Low voltage	≈(0.9-1.2)

In microgrid applications, the suitable droop control can be divided into three main types [18, 21]:

- Type-1: ($f - P, V - Q$), typical droop control used in inductive circuits.
- Type-2: ($V - P, Q - P$), reverse droop control used in resistive circuits.
- Type-3: ($P - V - f$), improved droop control used in resistive circuits.

It is important to point out that - in many cases - type-1 is implemented as a typical droop mechanism where its performance can be improved either by adding the virtual impedance or by placing a large and bulky coupling inductor to compensate for the high resistance [19, 26, 28].

3. THE PROPOSED DROOP CONTROL STRATEGY

To illustrate the configuration of the droop control and its implementation, Fig. 2 depicts a typical dual stage power electronics-based droop control system. Fig. 3 shows the power and control circuits of a grid connected DG system where the droop control is utilized to enable the grid forming mode of the DGs. The DGs are connected to the grid through an inductive coupling where the measured current and voltage signals are processed to obtain the actual active and reactive power values. The power signals are then filtered using a first order filter with a reasonable cutoff frequency.

The proposed droop control is applied by introducing the values of the droop coefficients. The general form of the proposed $f-P$ and $V-Q$ droop relations are given in Eqs. (5) and (6), respectively.

$$f_{out} = f_{nl} - \alpha_f \left(1 - \frac{P_{max} - P(t)}{P_{max}}\right)^{\beta_f} P(t) \tag{5}$$

$$V_{out} = V_{nl} - \alpha_v \left(1 - \frac{Q_{max} - Q(t)}{Q_{max}}\right)^{\beta_v} Q(t) \tag{6}$$

where $f_{nl}, V_{nl}, P(t),\ Q(t), P_{max}, Q_{max}$ are the no load frequency, no load voltage, output active power, output reactive power, maximum active power and the maximum reactive power, respectively. The performance of the proposed droop relations can be interpreted at different operating points as explained in Eq. (7) where X is the active/reactive power and Y is the frequency/voltage in the $f-P$and $V-Q$ droop relations, respectively. Therefore, as long as the power is within the operating range, the characteristics can be shaped according to the proposed relations. However, when the output power of the DG is maximum, the droop is solely determined by α_x where $\alpha_x = \alpha_f$ in $f-\ P$ droop and $\alpha_x = \alpha_v$ in $V-Q$ droop.

$$Y_{out} = \begin{cases} Y_{nl} & ,when\ X = 0 \\ Y_{nl} - \alpha_x \left(1 - \frac{X_{max} - X(t)}{X_{max}}\right)^{\beta_x} Y(t) & ,when\ 0 < X < X_{max} \\ Y_{nl} - \alpha_x X & ,when\ X = X_{max} \end{cases} \tag{7}$$

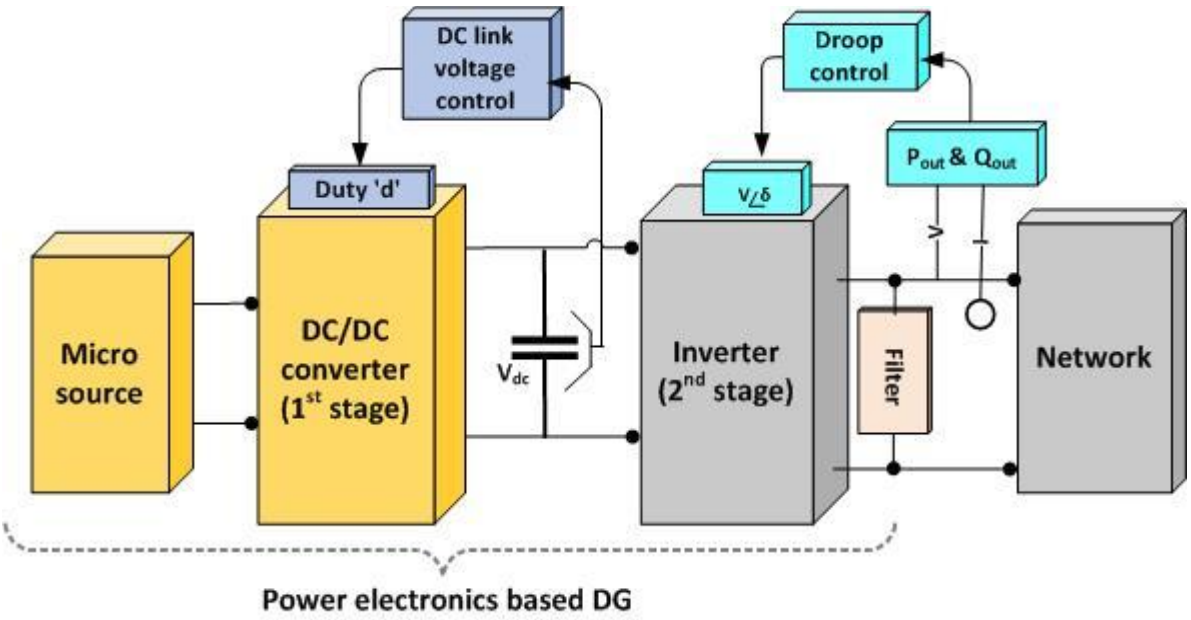

Fig. 2. Configuration of the dual stage droop-controlled DG.

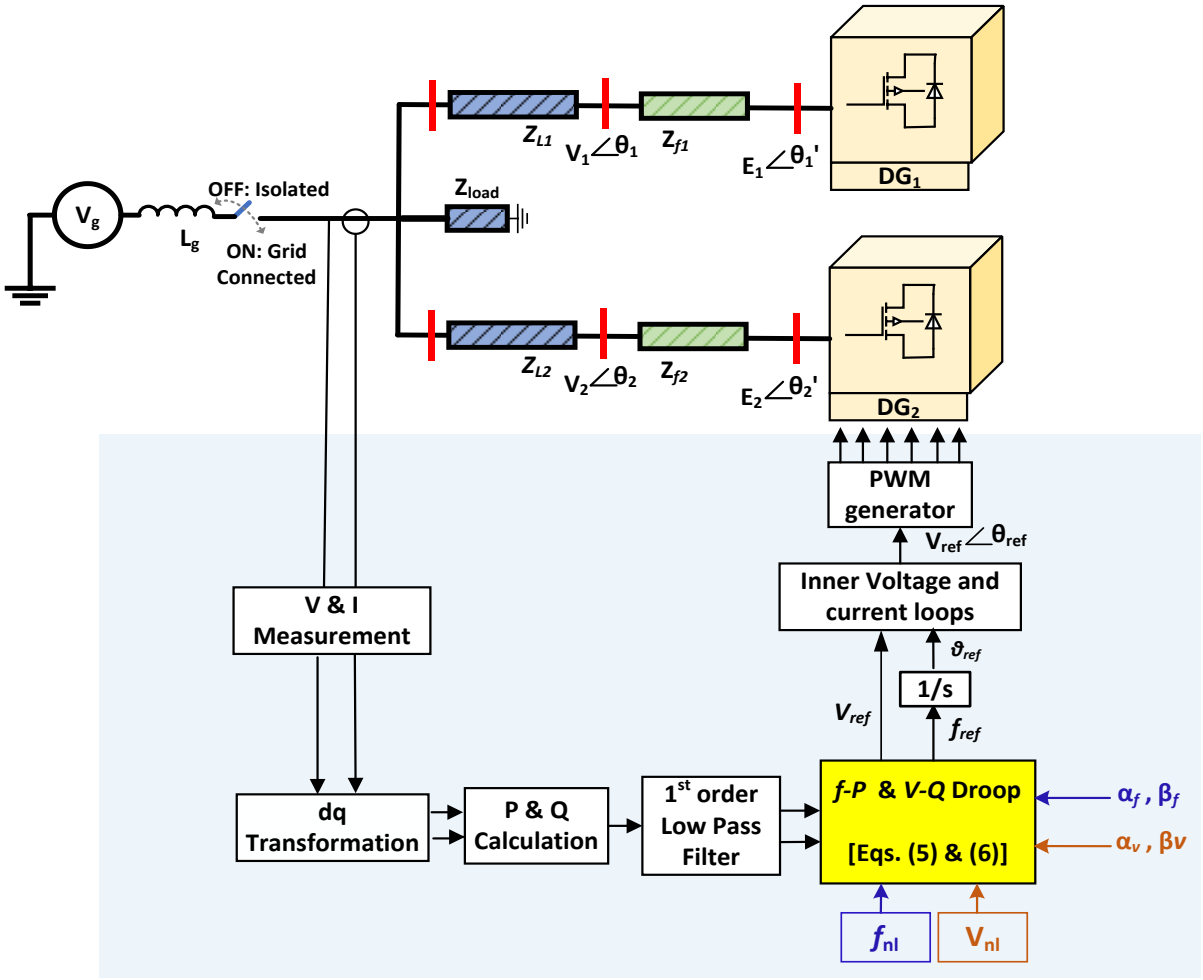

Fig. 3. Power-exponent droop-controlled grid connected DG.

The proposed frequency droop characteristics are depicted in Fig. 4(a) where the values of the coefficients are swept, independently, to cover all possible operating points. The figure shows how changing the coefficients can change the characteristics in both directions. As a result, the proposed droop would be used to fulfill complex multi-objective functions. For further visualization and illustration, the droop characteristics under negative β_f are separated in Fig. 4(b) whereas the characteristics with positive β_f are depicted in Fig. 4(c). The solid arrows in the figures show the direction of increasing β_f of each characteristic family at the corresponding α_f.

As can be seen from the characteristics depicted in Fig. 4, changing α_f dictates the maximum frequency variation (Δf) where the implemented characteristic is governed by the DG type, size and the maximum allowed power sharing of the DG. Compared to the linear droop characteristics, the proposed droop minimizes the frequency degradation of large size DGs under positive values of β_f for better frequency. This can be observed by comparing the frequency relations in Figs. 5(a) and 5(b) where at same value of output and maximum power (i.e., P_i and P_{max} in the figure) that DG can deliver, the frequency variation ($\Delta f = f_{ref} - f_{out}$) is less. This would be the same for the voltage variation where the proposed droop minimizes the voltage degradation in the $V - Q$ droop control.

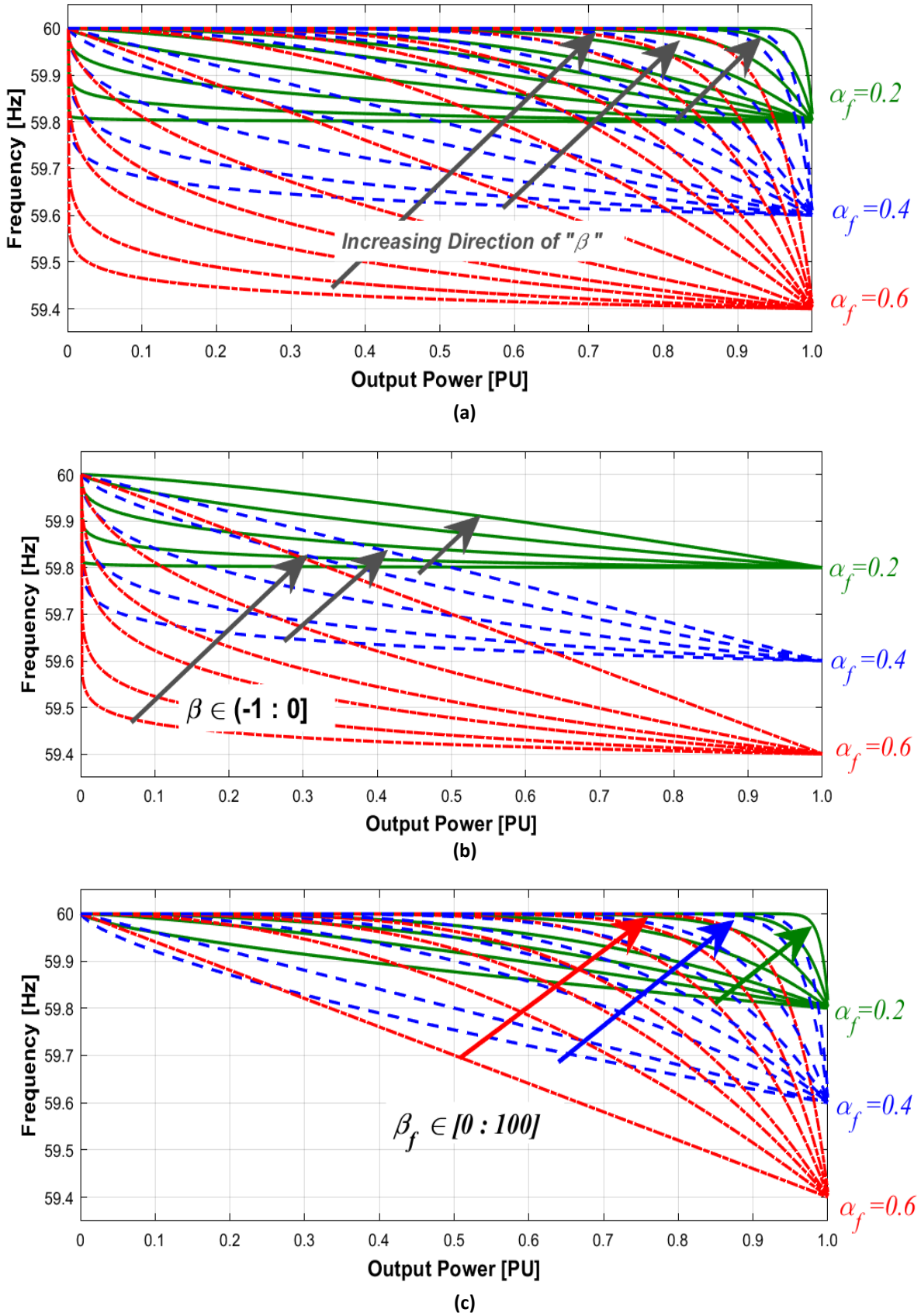

Fig. 4. Frequency droop characteristics of the proposed control strategy: a) the generated characteristics; b) the characteristics with negative β_f; c) the characteristics with positive β_f.

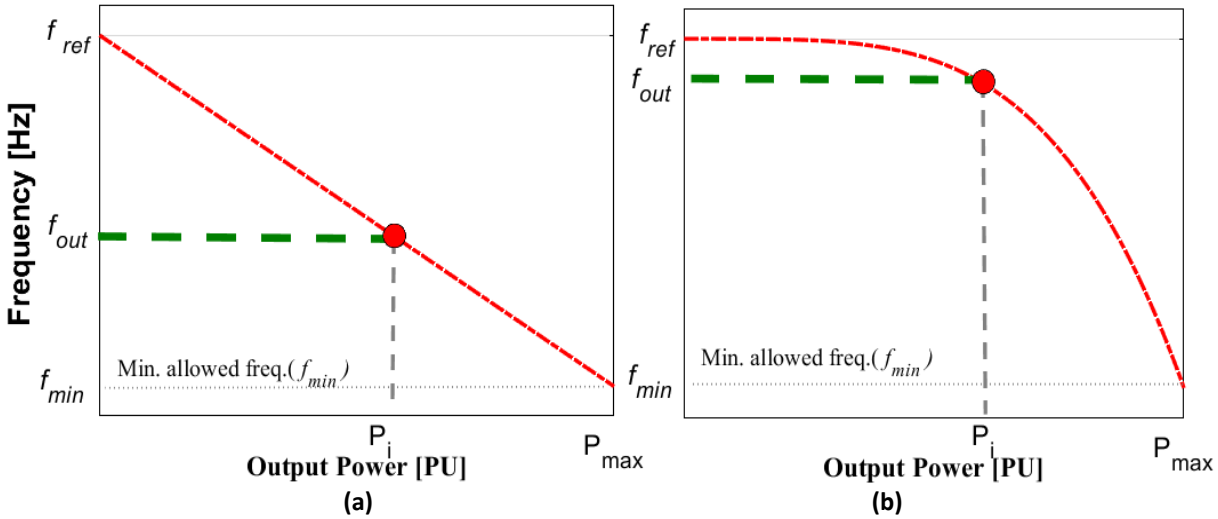

Fig. 5. Frequency relations for the: a) linear droop control; b) proposed droop control.

In a mixture of sources in a microgrid network, the right upper off-diagonal characteristics (i.e., with $\beta_f > 0$) are most likely to be adopted by DGs with large ratings as the operation approaches the semi-isochronous operation. This is because the flatness of the characteristics increases as shown in Fig. 6(b). On the other hand, the lower left off-diagonal (i.e., with $\beta_f < 0$) characteristics can be utilized by smaller rating DGs or dispatchable source as depicted in Fig. 6(c). If a dispatchable source is equipped with such characteristics (similar to Fig. 6(c)), it can automatically supply the extra demand in contingency situations before reaching the shedding point. Once the demand decreases or goes back to the scheduled amount, this source can be switched off automatically. This kind of source typically operates as an action against low frequency to restore the system frequency when under frequency problems happen.

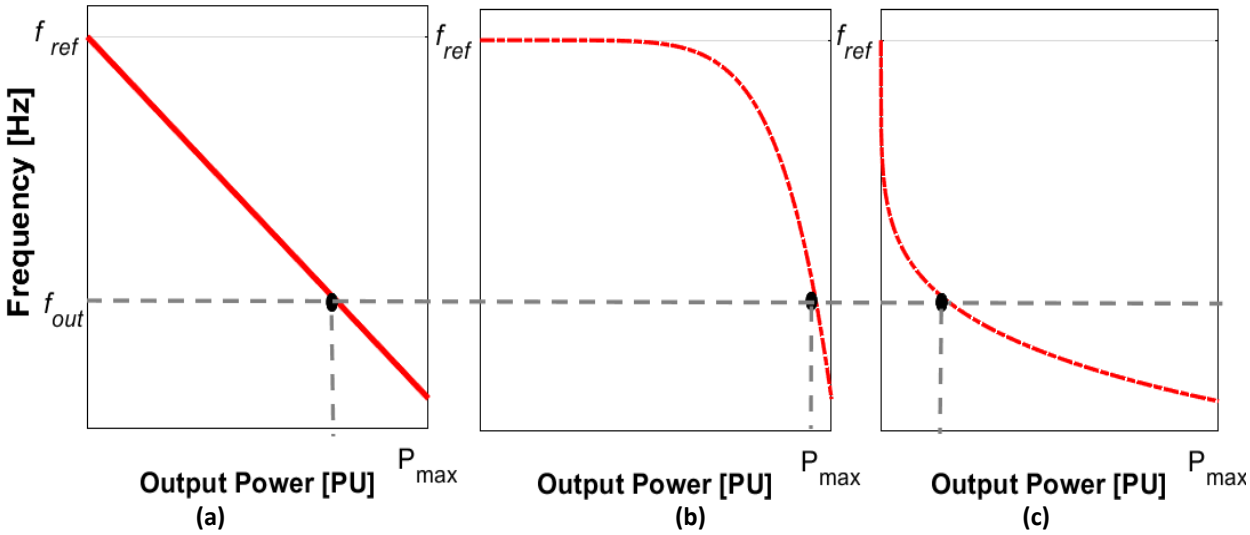

Fig. 6. Frequency relations for: a) typical linear droop control; b) large size DG/large power sharing; c) small power sharing / dispatchable source.

4. THE PROPOSED DROOP CONTROL VS. MAXIMUM POWER POINT TRACKING CONTROL

It is important to investigate the behavior of the proposed controller as a universal controller against the maximum power point tracking (MPPT) controller. This section discusses how the proposed control can efficiently work near the maximum power point (MPP) while maintaining the voltage and frequency stability.

MPPT control is a feedforward current control scheme used to maximize the available energy when employed in renewable energy sources interfaced to power network. Therefore, the connected DG can be characterized as a "grid feeding" DG where it doesn't provide any other services to the grid. On the other hand, the droop control is used as a feedback voltage control scheme utilized to stabilize the voltage of the system and characterized as a "grid forming" DG. Therefore, when a linear droop-controlled DG is connected to the utility grid, it helps regulating the voltage and injecting the power into the grid. However, this regulation restricts the DG from harvesting the whole available energy and imposes a reduced energy harvesting compared to MPPT control when equipped in a renewable source. The proposed droop when running under near-flat characteristics as shown in Fig. 7 can perform as a semi-MPPT control and keeps exporting the power to the grid with minimal effect on the voltage and frequency. The knee point of the curves represents the MPP. Therefore, a dynamic power headroom is flexibly allocated according to the generated characteristics. As a result, both the economic and technical objectives can be fulfilled when the proposed control is implemented in a renewable energy source.

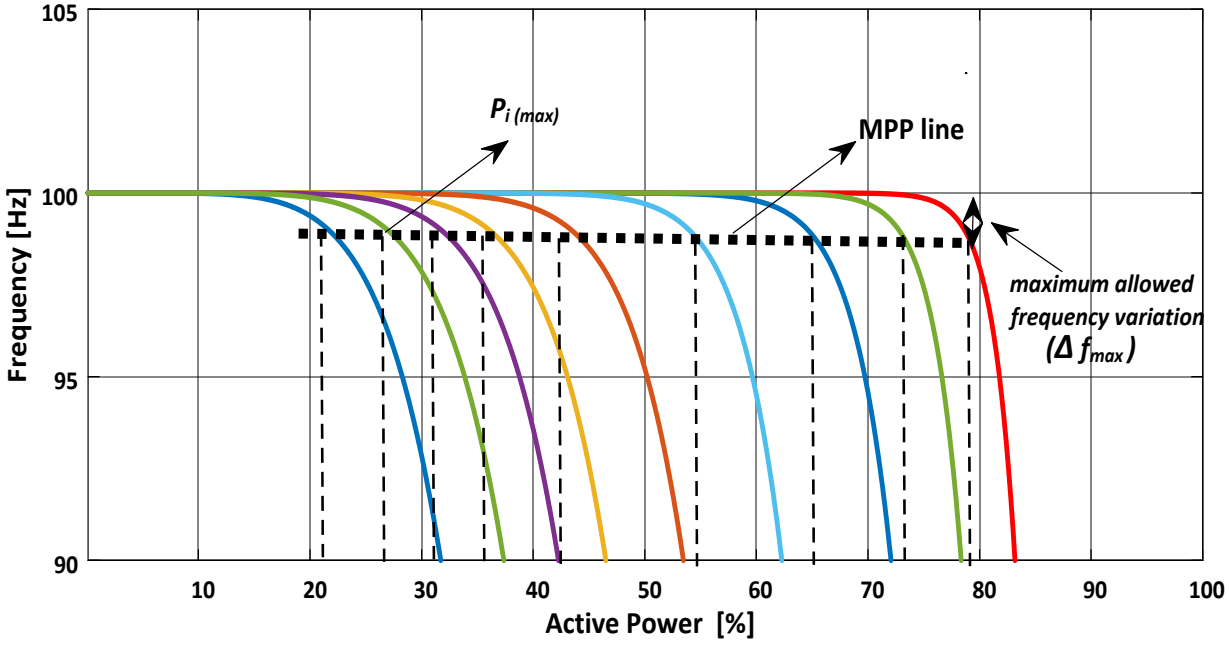

Fig. 7. The proposed droop control vs. MPPT.

5. SIMULATION RESULTS

The system given in Fig. 3 has been simulated in Matlab/Simulink to verify the proposed controller where two DGs are running in an islanded system. The system parameters are given in Table 2. Several cases have been considered to investigate the

applicability and the performance of the proposed control compared to the conventional linear droop control. Some cases are investigated on DGs with same ratings, and others are carried out on different DGs' rating to observe the effect of the proposed strategy on different DG capacity including different circuit parameters. In other cases, the proposed control is carried out to show the impact of the control parameters on the power sharing and voltage regulation of the network. A summary of the simulated scenario is given in Table 3.

Table 2. Parameters of the simulated system.

Parameters	Value
L_1 (mH)	Variable based on each case
L_{line1}(uH)	110
L_2(mH)	Variable based on each case
L_{line2} (uH)	100
R_1 ($\boldsymbol{\Omega}$)	1.2e-3
R_2 ($\boldsymbol{\Omega}$)	0.9e-3
V_{ref} (V)	120
f_{ref} (Hz)	60

Table 3. The simulated scenarios.

Case	Scenario	DG_1 control	DG_2 control
Case 1	Same rating DGs	Conventional	Proposed
Case 2	Different rating DGs	Conventional	Proposed
Case 3	Different rating DGs	Proposed	Proposed
Case 4	Variable α_f	Conventional	Proposed
Case 5	Variable β_f	Conventional	Proposed

Case 1: For this case, each DG size and the control applied on each DG are as given in Table 4. Here, both DGs have the same ratings. A step load change is inserted at t = 1.0 s.

Table 4. System parameters for case 1.

DG	Control type	DG capacity	inductor size	Control parameters
DG_1	Conventional	5 kW	3 mH	m_p=4.5e-5 Hz/W
DG_2	Proposed	5 kW	3 mH	$\alpha = 0.22$ Hz/W, $\beta = 3$

Four main results are considered for the comparison purposes, namely the shared active and reactive power of each source, the output frequency and the output voltage of each DG. The results of this case are given in Fig. 8 where both DGs equally share the load under different control strategies. The results show that the proposed controller performs well under different loading conditions. Moreover, the proposed control strategy can command the DG to equalize the power sharing and stabilize the performance under different operating conditions.

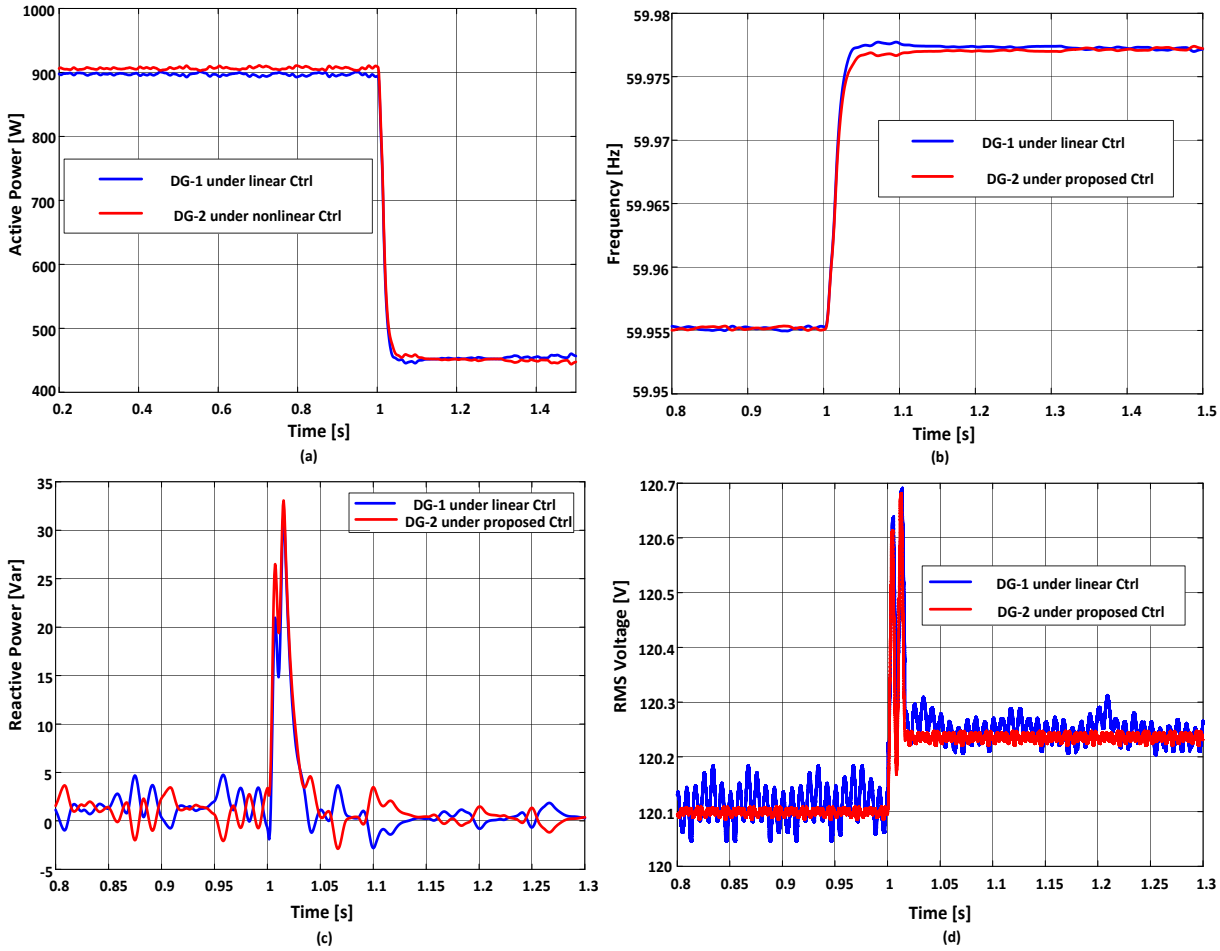

Fig. 8. The results of case 1 when a step load change occurs at t =1s: a) the power sharing between the DGs; b) the frequency signal of each DG; c) the reactive power sharing between the DGs; d) the load rms voltage.

Case 2: For this case, each DG size and the control applied on each DG are as given in Table 5. The proposed control is implemented on DG_2, and the conventional linear droop is applied on DG_1.

Table 5. System parameters for case 2.

DG	Control type	DG capacity	Inductor size	Control parameters
DG_1	Conventional	5 kW	3 mH	m_p=4.5e-5 Hz/W
DG_2	Proposed	3 kW	2 mH	$\alpha = 0.2$ Hz/W, $\beta = -0.32$

The results of this case are compared with the conventional droop as depicted in Fig. 9. To clarify the comparison, the case where both DGs run under linear droop are shown to observe the difference of DG_2 performance under both controllers. The plots compare the dynamic power sharing, the frequency profile, the reactive power sharing and the bus voltage of each DG before and after implementing the proposed control on DG_2. It is clear that the proposed droop positively impacts the steady state and transient performance of the DG and minimizes the maximum frequency deviation during a step load change. As the subplots show that the proposed control stabilizes the performance of DG_2 and yields less frequency variation under load step change.

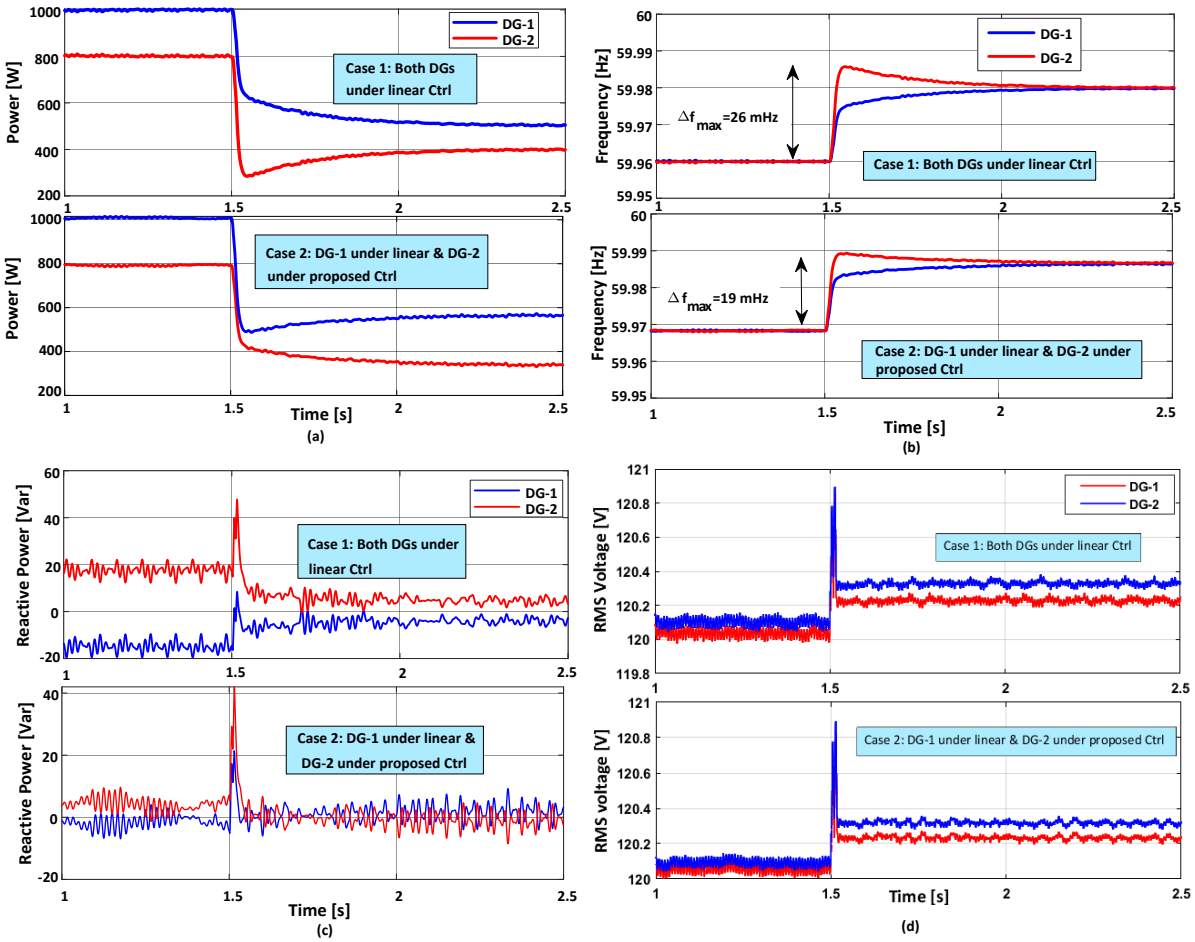

Fig. 9. The results of case 2 when a step load change occurs at t =1 s: a) the power sharing between the DGs; b) the frequency of each DG; c) the reactive power sharing between the DGs; d) the load rms voltage.

Case 3: For this case, the proposed control is implemented on both DGs to show how adaptively the load can be shared between the DGs. The DG size and the applied control are as given in Table 6. The results depicted in Fig. 10 show that the proposed control can adaptively share the power; where the power ratio between the DGs is variable under different loadings. In Fig. 10(b), the power ratio shows that the power of DG_1 varies from about zero to 60% of the power shared by DG_2.

Table 6. System parameters for case 3.

DG	Control type	DG capacity	Filter inductor Size	Control parameters
DG_1	Proposed	3 kW	2 mH	$\alpha = 0.2$ Hz/W, $\beta = 0.5$
DG_2	Proposed	5 kW	3 mH	$\alpha = 0.2$ Hz/W, $\beta = 3$

Case 4: In this case, the droop coefficient, α_f, is swept to reflect the impact of the gradient/slope variation of the curve on the power sharing. Different reasonable values of α_f are considered while keeping the droop coefficient $\beta_f = -0.2$. The power sharing and frequency waveforms obtained in this part are depicted in Fig. 11. It can be seen from the plots that α_f has a significant effect on shifting the power output of the DG.

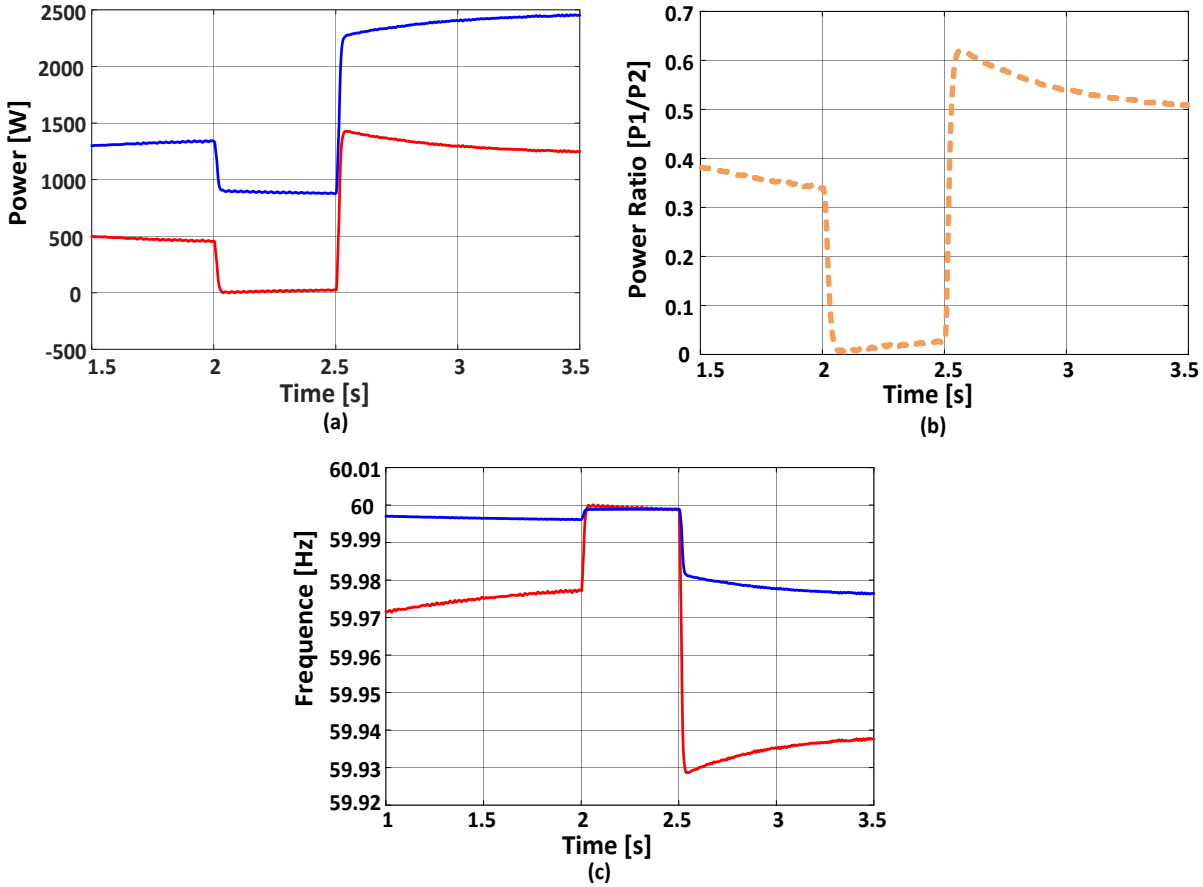

Fig. 10. The results of case 3: a) the adaptive power sharing; b) the power ratio [%]; c) the frequency of each DG.

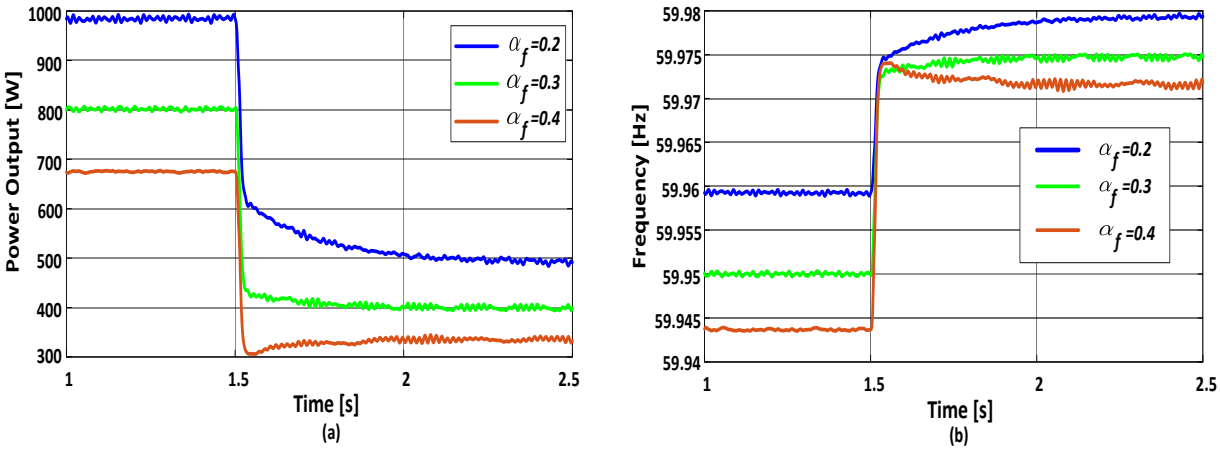

Fig. 11. The results of case 4: a) the power output of DG_2; b) the frequency of DG_2.

Case 5: This case is considered to express the impact of the nonlinearity degree of the droop characteristics on the power sharing of the DGs. Different values of the droop coefficient, β_f, are considered while keeping $\alpha_f = 0.2$. The power sharing and frequency waveforms obtained are depicted in Fig. 12. It can be seen from the plots that β_f has a significant effect on dynamically shifting the power output of the DG. Comparing Fig. 11 with Fig. 12 shows that both coefficients play a major role in shaping the relations. This, in turn, increases the degree of freedom in controlling the power of the DGs under all operating conditions.

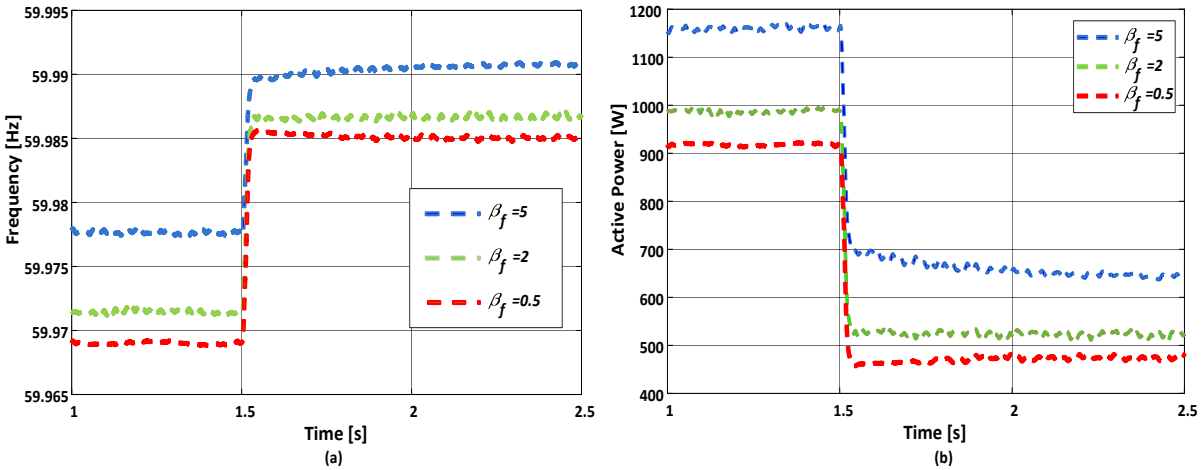

Fig. 12. The results of case 5: a) the power output of DG_2; b) the frequency of DG_2.

6. CONCLUSIONS

This paper proposed a simple but effective control mechanism that can be easily implemented to achieve multiple design objectives and flexible operations. The proposed droop control can be considered as a universal control strategy due its ability to cover the whole area in $f - P$ plane. Therefore, numerous operating trajectories can be realized to fulfill any complex design requirements. The proposed droop was implemented into microgrid network and compared to the conventional droop control to verify its effectiveness. The results showed the superiority of the proposed droop control in controlling the DGs under different operating conditions. It is important to mention that the proposed droop was applied on $f - P$ relation and will be applied on $V - Q$ relation in a future work.

REFERENCES

[1] J. Lopes, C. Moreira, A. Madureira, "Defining control strategies for microgrids islanded operation," *IEEE Transactions on Power Systems*, vol. 21, no. 2, pp. 916–924, 2006.

[2] J. Guerrero, J. Vasquez, J. Matas, L. de Vicuna, M. Castilla, "Hierarchical control of droop-controlled AC and DC microgrids–a general approach toward standardization," *IEEE Transactions on Industrial Electronics*, vol. 58, no. 1, pp. 158–172, 2011.

[3] D. Olivares, A. Mehrizi-Sani, A. Etemadi, C. Canizares, R. Iravani, M. Kazerani, A. Hajimiragha, O. Gomis-Bellmunt, M. Saeedifard, R. Palma-Behnke, G. Jimenez-Estevez, N. Hatziargyriou, "Trends in microgrid control," *IEEE Transactions on Smart Grid*, vol. 5, no. 4, pp. 1905–1919, 2014.

[4] Q. Zhong, T. Hornik, *Control of Power Inverters in Renewable Energy and Smart Grid Integration*, Wiley-IEEE Press, 2013.

[5] Z. Li, K. Chan, J. Hu, J. Guerrero, "Adaptive droop control using adaptive virtual impedance for microgrids with variable PV outputs and load demands," *IEEE Transactions on Industrial Electronics*, vol. 68, no. 10, pp. 9630-9640, 2021.

[6] J. Simpson-Porco, F. Dörfler, F. Bullo, "Voltage stabilization in microgrids via quadratic droop control," *IEEE Transactions on Automatic Control*, vol. 62, no. 3, pp. 1239-1253, 2017.

[7] L. Zhang, H. Zheng, Q. Hu, B. Su, L. Lyu, "An adaptive droop control strategy for islanded microgrid based on improved particle swarm optimization," *IEEE Access*, vol. 8, pp. 3579-3593, 2020.

[8] B. Alghamdi, C. Cañizares, "Frequency regulation in isolated microgrids through optimal droop gain and voltage control," *IEEE Transactions on Smart Grid*, vol. 12, no. 2, pp. 988-998, 2021.

[9] S. Ahmadi, S. Shokoohi, H. Bevrani, "A fuzzy logic-based droop control for simultaneous voltage and frequency regulation in an AC microgrid," *International Journal of Electrical Power and Energy Systems*, vol. 64, pp. 148-155, 2015.

[10] J. Mueller, J. Kimball, "An efficient method of determining operating points of droop-controlled microgrids," *IEEE Transactions on Energy Conversion*, vol. 32, no. 4, pp. 1432-1446, 2017.

[11] M. Abdelaziz, H. Farag, E. El-Saadany, "Optimum droop parameter settings of islanded microgrids with renewable energy resources," *IEEE Transactions on Sustainable Energy*, vol. 5, no. 2, pp. 434-445, 2014.

[12] A. Saleh-Ahmadi, M. Moattari, A. Gahedi, E. Pouresmaeil, "Droop method development for microgrid control considering higher order sliding mode control approach and feeder impedance variation," *Applied Sciences*, vol. 11, no. 3, pp. 967 2021.

[13] F. Zandi, B. Fani, A. Golsorkhi, "A visually driven nonlinear droop control for inverter-dominated islanded microgrids," *Electrical Engineering*, vol. 102, no. 3, pp. 1207–1222, 2020.

[14] A. Anvari-Moghadam, Q. Shafiee, J. Vasquez, J. Guerrero, "Optimal adaptive droop control for effective load sharing in AC microgrids," *IECON 2016 - 42nd Annual Conference of the IEEE Industrial Electronics Society*, pp. 3872-3877, 2016.

[15] R. Lin, M. Yang, H. Li, "Analysis of parallel photovoltaic inverters with improved droop control method," *International Conference on Modelling, Simulation and Applied Mathematics*, pp. 84-88, 2015.

[16] S. Harasis, Y. Sozer, "Improved transient power sharing of droop controlled islanded microgrids," *2020 IEEE Applied Power Electronics Conference and Exposition*, pp. 2346-2351, 2020.

[17] C. Li, S. Chaudhary, M. Savaghebi, J. Quintero, J. Guerrero, "Power flow analysis for low-voltage AC and DC microgrids considering droop control and virtual impedance," *IEEE Transactions on Smart Grid*, vol. 8, no. 6, pp. 2754-2764, 2017.

[18] M. Azim, M. Hossain, H. Pota, "Design of a controller for active power sharing in a highly-resistive microgrid," *IFAC-PapersOnLine*, vol. 48, no. 30, pp. 288-293, 2015.

[19] Z. Liu, S. Ouyang, W. Bao, "An improved droop control based on complex virtual impedance in medium voltage micro-grid," *2013 IEEE PES Asia-Pacific Power and Energy Engineering Conference*, pp. 1-6, 2013.

[20] A. Kahrobaeian, Y. Mohamed, "Stability analysis and control of medium-voltage micro-grids with dynamic loads," *2013 IEEE Power and Energy Society General Meeting*, pp. 1-5, 2013.

[21] E. Rokrok, M. Shafie-khah, J. Catalão, "Review of primary voltage and frequency control methods for inverter-based islanded microgrids with distributed generation," *Renewable and Sustainable Energy Reviews*, vol. 82, pp.3225-3235, 2018.

[22] S. Harasis, K. Mahmoud, S. Albatran, K. Alzaareer, Q. Salem, "Dynamic performance evaluation of inverter feeding a weak grid considering variable system parameters," *IEEE Access*, vol. 9, pp. 126104-126116, 2021.

[23] S. Harasis, H. Abdelgabir, Y. Sozer, M. Kisacikoglu, A. Elrayyah, "A center of mass determination for optimum placement of renewable energy sources in microgrids," *IEEE Transactions on Industry Applications*, vol. 57, no. 5, pp. 5274-5284, 2021.

[24] Y. Ashraf, N. Elsobky, M. Hamouda, M. Sabry, S. Kaddah, B. Badr, "Controlling single-stage and quasi-resonant flyback converters for solar power systems," *Jordan Journal of Electrical Engineering*, vol. 7, no. 2, pp. 148-165, 2021.

[25] D. Dinakin, P. Oluseyi, "Optimal under-frequency load curtailment via continuous load control in a single area power system using fuzzy logic, PID-fuzzy and neuro-fuzzy (ANFIS) Controllers," *Jordan Journal of Electrical Engineering*, vol. 4, no. 4, pp. 208-223, 2018.

[26] Y. Han, H. Li, P. Shen, E. Coelho, J. Guerrero, "Review of active and reactive power sharing strategies in hierarchical controlled microgrids," *IEEE Transactions on Power Electronics*, vol. 32, no. 3, pp. 2427-2451, 2017.

[27] M. Legha, S. Rashidifard, "Energy management in multiple micro-grids considering uncertainties of load using hierarchical multi-agent system," *Jordan Journal of Electrical Engineering*, vol. 7, no. 2, pp. 166-178, 2021.

[28] M. Kreishan, A. Zobaa, "Optimal allocation and operation of droop-controlled islanded microgrids: a review," *Energies*, vol. 14, no. 15, pp. 4653, 2021.